Arch. Min. Sci. **65** (2020), 3, 469-491

Electronic version (in color) of this paper is available: http://mining.archives.pl

DOI 10.24425/ams.2020.134130

ANDRZEJ PYTLIK[1*]

EXPERIMENTAL STUDIES OF STATIC AND DYNAMIC STEEL ARCH SUPPORT LOAD CAPACITY AND SLIDING JOINT TEMPERATURE PARAMETERS DURING YIELDING

Difficult geological and mining conditions as well as great stresses in the rock mass result in significant deformations of the rocks that surround the workings and also lead to the occurrence of tremors and rock bursts. Yielding steel arch support has been utilised in the face of hard coal extraction under difficult conditions for many years, both in Poland and abroad. A significant improvement in maintaining gallery working stability is achieved by increasing the yielding support load capacity and work through bolting; however, the use of rock bolts is often limited due to factors such as weak roof rock, significant rock mass fracturing, water accumulation, etc. This is why research and design efforts continue in order to increase yielding steel arch support resistance to both static and dynamic loads. Currently, the most commonly employed type of yielding steel arch support is a support system with frames constructed from overlapping steel arches coupled by shackles. The yield of the steel frame is accomplished by means of sliding joints constructed from sections of various profiles (e.g. V, TH or U-type), which slip after the friction force is exceeded; this force is primarily dependent on the type of shackles and the torque of the shackle screw nuts.

This article presents the static bench testing results of ŁP10/V36/4/A, ŁP10/V32/4/A and ŁP10/V29/4/A yielding steel arch support systems formed from S480W and S560W steel with increased mechanical properties. The tests were conducted using 2 and 3 shackles in the joint, which made it possible to compare the load capacities, work values and characteristics of various types of support. The following shackle screw torques were used for the tests:

- M_d = 500 Nm – for shackles utilised in the support constructed from V32 and V36 sections.
- M_d = 400 Nm – for shackles utilised in the support constructed from V29 sections.

The shackle screw torques used during the tests were greater compared to the currently utilised standard shackle screw torques within the range of M_d = 350-450 Nm.

Dynamic testing of the sliding joints constructed from V32 section with 2 and 3 shackles was also performed. The SD32/36W shackles utilised during the tests were produced in the reinforced versions and manufactured using S480W steel.

[1] CENTRAL MINING INSTITUTE, 1 GWARKÓW SQ., 40-166 KATOWICE, POLAND

* Corresponding author: ja.pytlik@gmail.com

Since comparative testing of a rock bolt-reinforced steel arch support system revealed that the bolts would undergo failure at the point of the support yield, a decision was made to investigate the character of the dynamics of this phenomenon. Consequently, this article also presents unique measurement results for top section acceleration values registered in the joints during the conduction of support tests at full scale.

Filming the yield in the joint using high-speed video and thermal cameras made it possible to register the dynamic characteristics of the joint heating process at the arch contact point as well as the mechanical sparks that accompanied it. Considering that these phenomena have thus far been poorly understood, recognising their significance is of great importance from the perspective of occupational safety under the conditions of an explosive atmosphere, especially in the light of the requirements of the new standard EN ISO 80079-36:2016, harmonised with the ATEX directive.

Keywords: yielding steel arch support; support shackle torque; static and dynamic load capacity; support work; arch acceleration in sliding joints; joint sparking and heating temperature during yielding

1. Introduction

The necessity of conducting hard coal deposit extraction at increasingly greater depths in Polish mines [1,2] has resulted in an increase in hazards related to the loss of stability of the working support. Currently, hard coal deposits in Poland are already being mined at a depth of 1290 m. Difficult geological and mining conditions as well as the great stresses in the rock mass result in significant deformations of the rocks that surround the workings [3] and also lead to the occurrence of tremors and rock bursts [4-8]. Yielding steel arch support has been utilised in the face of hard coal extraction under difficult conditions for many years both in Poland and globally [9-21]. A significant improvement in maintaining gallery working stability is achieved by increasing the yielding support load capacity and work through bolting [16,22-26]. However, the use of rock bolts is often limited due to unfavourable roof conditions. Some limitations are also imposed by the different character of the interaction of the yielding steel arch support and the bolts (which typically constitute rigid support) with the rock mass [20,27]. That is why research and design efforts continue in order to increase the yielding steel arch support resistance to both static and dynamic loads.

Tests of yielding steel arch support element resistance to static loads, with and without reinforcement by means of rock bolts, are conducted at the Central Mining Institute's test facility in Katowice. The support and shackle tests are carried out at full scale, according to Polish standards [28-33].

Resistance tests of yielding steel arch support elements (sliding joints) and rock bolts to dynamic loads are conducted at the Central Mining Institute's test facility in Łaziska Górne by means of the dynamic impact drop test [18,34,35].

The basic type of gallery working support is the yielding steel arch support [28,36-38] constructed from overlapping arched elements coupled by shackles.

The yield of the steel frame is accomplished by means of sliding joints constructed from sections of various profiles (e.g. V, TH or U-type), which slip after the friction force is exceeded; this force is primarily dependent on the type of shackles and the torque of the shackle screw nuts [17,39-46].

This article presents the static bench testing results of ŁP10/V36/4/A, ŁP10/V32/4/A and ŁP10/V29/4/A yielding steel arch support systems formed from S480W [31] and S560W steel with increased mechanical properties. The tests were conducted using 2 and 3 shackles in the joint, which made it possible to compare the load capacities, work values and characteristics of various types of support.

The shackle screw torques used during the tests were greater compared to the currently utilised standard shackle screw torques which are within the range of M_d = 300-450 Nm [12,13,42,43]. Dynamic testing of the sliding joints formed from V32 sections with 2 and 3 shackles was also performed. Reinforced versions of the SD36W shackles utilised during the tests were produced as well, and they were manufactured using S480W steel.

Since comparative testing of a rock bolt-reinforced steel arch support system, the results of which are presented in detail in literature [24], revealed that the bolts would undergo failure at the point of the support yield, a decision was made to investigate the character of the dynamics of this phenomenon. Thus, this article also presents selected top section acceleration measurement results registered in the joints during yielding.

As mechanical sparking at yield is observed during static support frame testing, measurements using a high-speed thermal camera were also carried out. Data regarding the temperature distribution in the joint during yielding may prove conducive to detecting the locations that influence the increase in frictional resistance, and consequently to increasing the support frame load capacity. Determining the maximum surface temperature generated during yielding will make it possible to verify whether it exceeds the temperature defined in standard EN ISO 80079-36:2016 [47], which is harmonised with the ATEX directive concerning group I non-electrical equipment intended for use under the conditions of explosive atmospheres. Some of the aspects defined in the standard include the maximum temperature T = 150°C for a surface that can accumulate a layer of coal dust.

2. Test results and analysis

The analysis of support types [2] employed in development headings in the mines belonging to Jastrzębska Spółka Węglowa (JSW SA – the largest producer of coking coal in the European Union) identifies the ŁP-type yielding steel arch support as the most frequently used support system. Currently, the greatest extraction depth in the JSW SA mines reaches 1290 m. The greatest tremor in recent times was registered in the KWK BUDRYK mine, and its magnitude reached 4 degrees on the Richter scale (registered by the Upper Silesian Seismological Network of the Central Mining Institute in Katowice (GRSS-EPOS)). The dominant support frame sizes are 9 and 10, while the most often used section sizes are (respectively): V32, V29 and V36. The sections are mostly formed from standard 25G2 steel (PN-89/H-84023/05/Az2) with a minimum strength of R_e = 340 MPa and R_m = 550 MPa at A_5 = 18%. However, due to the constantly deteriorating geological and mining conditions, grades of steel with greater ductility and increased mechanical properties have seen increased application in recent times, such as S480W steel (R_e = 480 MPa and R_m = 650 MPa at A_5 = 17%) according to standard PN-H-84042: 2009/Az1:2012 or S550W steel (R_e = 550 MPa and R_m = 730 MPa at A_5 = 18%) manufactured according to internal standard ZN/TT/2012/1. S560W steel currently exhibits the greatest strength among non-toughened grades of steel used for support frame sections, and its minimum strength is R_e = 560 MPa and R_m = 740 MPa (Specifications no. WT/S1/J.207). Yet the actual strength of S560W steel, e.g. used for a V32 section, significantly exceeds the minimum strength values defined in the specifications, and it can reach R_e = 599 MPa and R_m = 793 MPa at an elongation of A_5 = 21.1% and impact strength KCU2A = 92.0 J/cm^2 (Acceptance certificate no. BDO:000012617 of 28.08.2019).

2.1. Support frame test results under static loading

Based on the above analysis, size-10 support frames (height H = 3.8 m, width W_F = 5.5 m, cross sectional area approx. 17.8 m^2) of the following types were selected for testing: ŁP10/V36/4/A, ŁP10/V32/4/A and ŁP10/V29/4/A [48] formed from S480W and S560W steel (Specifications no. WT/S1/J.207). All the tested frames were composed of four arched sections: two top sections and two side sections. 20 support frames were tested in total, with five pieces of each type of frame and grade of steel.

The yielding support frame bench testing was conducted at the Central Mining Institute's test facility in Katowice, displayed as a diagram in Fig. 1. Active (F_4, F_5, F_6) and passive (F_1, F_2, F_3, F_7, F_8, F_9) forces were exerted on the support by means of hydraulic actuators.

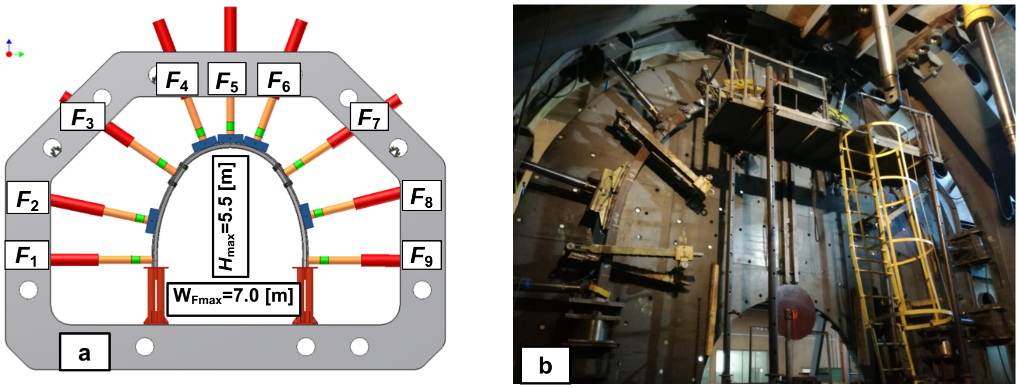

Fig. 1. Frame loading method according to Polish standard PN-G-15022:2018-11 during bench testing: a – test diagram; b – picture of the frame in the test facility

The test facility makes it possible to control each hydraulic actuator individually (independently), but according to the requirements of Polish standard PN-G-15022:2018-11, the roof-side loading (actuators F_4, F_5 and F_6) constitutes active loading, whereas the side loading (actuators F_1, F_2, F_3, F_7, F_8, F_9) constitutes passive loading. The test facility is also employed to conduct closed support system testing when equipped with additional actuators exerting active load (F_{10}, F_{11} and F_{12}) from the direction of the floor. Adopting the load diagram defined in the standard makes it possible to compare various types of support systems based on the conducted tests. In special cases (e.g. at the request of a mining plant or support manufacturer, or as part of legal procedures undertaken as a result of an accident), support tests may be conducted under asymmetric loading, with any configuration of active and passive loads. For the purposes of the comparative tests presented in this article, the operation of the hydraulic actuators that exert active and passive load was improved, and the active actuator load rates were equalised. This made it feasible to load the steel support frames as closely as possible to the vertical plane where the top and side support sections are located.

The ŁP10/V32/4/A support frames were formed from S480W and S560W grades of steel with increased mechanical properties, whereas the ŁP10/V36/4/A and ŁP10/V29/4/A frames were formed from S480W steel. The tests were conducted using 2 and 3 shackles in the joint. This made it possible to determine the influence of various mechanical parameters on the support load capacity and the work. Reinforced SD36W and SDO29W shackles were used for coupling the support frame sections during the tests. The shackles were manufactured using S480W steel, and their dimensions were compliant with the applicable standard (PN-G-15011:2011).

SD36W double-clevis shackles (reinforced versions) produced according to standard PN-G-15011:2011 were used for coupling the ŁP10/V36/4/A and ŁP10/V32/4/A support frame sections. These shackles are comprise of a lower and upper clevis, coupled using two special grade 10.9 M24 screws with grade 10 nuts. The SDG36W upper shackle together with the SDD36W lower shackle are intended for coupling support frame elements constructed from V32, V34 or V36 sections. The SDS36W middle shackle is used as a third, additional shackle in such joints. It is comprised of an upper clevis from an SDG36W shackle and a lower clevis from an SDD36W shackle.

SDO29W double-clevis shackles (reinforced versions) produced according to standard PN-G-15011:2011 were used for coupling the ŁP10/V29/4/A support frame sections. These shackles are comprised of a lower and upper clevis, coupled using two special grade 10.9 M24 screws with grade 10 nuts.

The shackle screw torques used during the tests were greater compared to the currently utilised standard torques of M_d = 350-450 Nm:

- M_d = 500 Nm – for shackles utilised in the support constructed from V32 and V36 sections.
- M_d = 400 Nm – for shackles utilised in the support constructed from V29 sections.

A set of SD36W double-clevis shackles in one joint is comprised of either:

- 2 shackles: upper and lower
- 3 shackles: upper, lower and middle.

Each shackle is equipped with two special M24 screws of mechanical property grade 10.9 and two special grade 10 M24 nuts.

Dynamic tests of joints constructed from V32 and V29 sections were conducted in order to determine the influence of the third shackle on the sliding joint load capacity.

As per the applicable standard, the frames were tested in rigid and yielding states.

The rigid support frame testing methodology consists of loading the frame according to the diagram provided in Fig. 1 until a 20% decrease in the force F ($F = F_4 + F_5 + F_6$) is achieved compared to the maximum load F_{max}.

The yielding support frame testing methodology consists of loading the frame according to the same diagram until one of the following effects is achieved:

- the frame height decreases by a total value of 300 mm as a result of joint yield,
- the frame joints jam,
- any support element becomes damaged.

In addition to the support frame parameters, as required by the standard and related to force and displacement measurements, the support work W value was also calculated, by means of numerical integration (trapezoidal rule), in order to compare the various types of frames, using the following formula:

$$W = \int_{H_1}^{H_2} F(H)\, dH, \text{kJ} \tag{1}$$

where:

- F — measured loading force, kN
- H — support frame height reduction ranging from $H_1 = 0$ to a value of H_2 [m] achieved by the conclusion of the test.

The test facility was equipped with two QUANTUM$^{X.}$ measuring amplifiers. Both the amplifiers were synchronised in time. One of them was connected to strain gauge pressure sensors installed in the hydraulic actuators that exerted the active load on the support frame and to displacement sensors measuring the support frame height reduction and the yield in the joints. The recording of these parameters was accomplished with a sampling frequency within the range of f_s = 1-10 Hz. The other measuring amplifier was connected to a B12/2000 inductive accelerometer with a measuring range of ±2500 m/s^2. Initially, the recording was conducted at a signal sampling frequency of f_s = 19200 Hz, but subsequent experiments demonstrated that the optimal sampling frequency was already reached at f_s = 4800 Hz, which was sufficient to ensure an accelerometer bandwidth within 0-1000 Hz.

A high-speed thermal camera with an accuracy of ±2°C and sampling frequency of 128 Hz that allowed the recording of phenomena within a temperature range of 0-250°C was used to register the location of mechanical sparking occurring during yielding and the temperature distribution in the sliding joint. Afterwards, the recorded temperature was compared to the requirements of standard EN ISO 80079-36:2016 harmonised with the ATEX directive concerning group I non-electrical equipment intended for use under the conditions of explosive atmospheres. The criterion value defined in this standard is a maximum temperature T = 150°C for a surface that can accumulate a layer of coal dust.

2.1.1. ŁP10/V32/4/A support frame test results

Fig. 2 presents the test courses of ŁP10/V32/4/A support frames formed from S480W steel in rigid and yielding states, including the value of support work W.

The maximum load capacity of the rigid ŁP10/V32/4/A support frame formed from S480W steel (Fig. 2a) was $F_{\max}$ = 1069 kN, while the support frame work at the end of the test was approx. W = 130 kJ. Tests have shown that it is possible to determine the rigid support frame load capacity characteristics $F = f(\Delta H)$ using a mathematical function, and the correlation between it and the experimental course is very high. A given characteristic $F = f(\Delta H)$ in the form of a square function can therefore be used for numerical simulations when modelling support load capacity. The maximum load capacity of the yielding ŁP10/V32/4/A support frame formed from S480W steel (Fig. 2b, c and d) was $F_{N\max}$ = 714 kN with two shackles and $F_{N\max}$ = 847 kN with three shackles. The work value after a support frame height reduction by approx. DH = 300 mm was approx. W = 120 kJ (with two shackles) and approx. W = 150 kJ (with three shackles).

An important feature of the support frame load capacity characteristic is its first stage, when the load capacity is approximated within a frame height reduction range of up to ΔH = 100 mm [24].

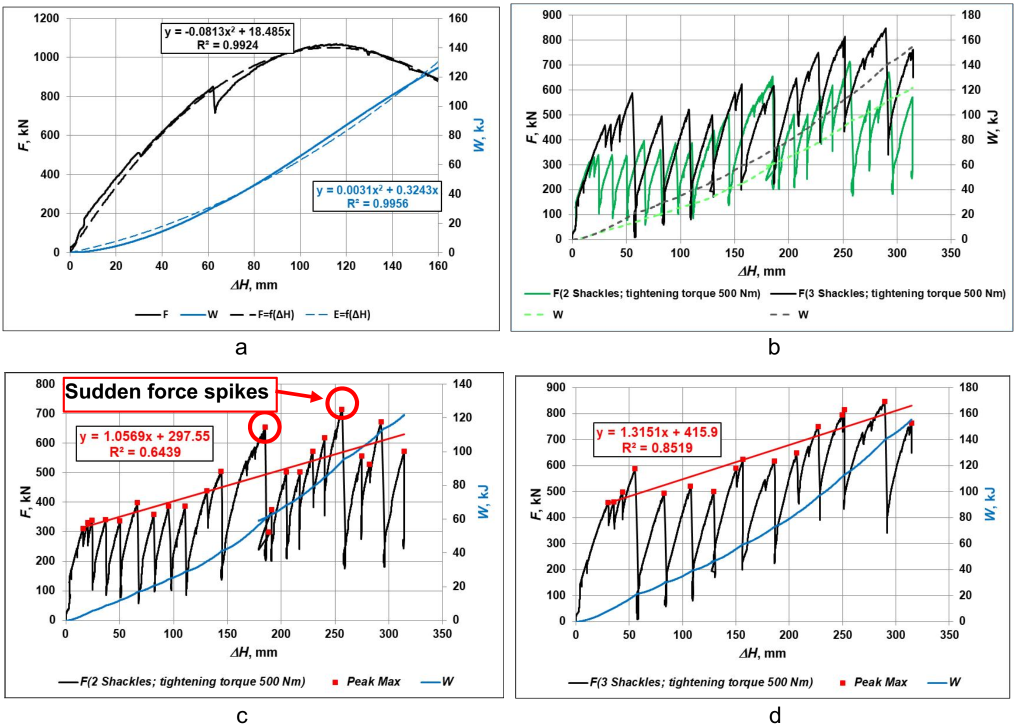

Fig. 2. Test courses of ŁP10/V32/4/A frames formed from S480W steel in various states: a – rigid (F_{max} = 1069 kN); b – yielding: load capacity comparison for frames with 2 and 3 shackles; c – yielding with 2 shackles ($F_{N\max}$ = 714 kN); d – yielding with 3 shackles ($F_{N\max}$ = 847 kN)

The load capacity comparison chart for frames with 2 and 3 shackles demonstrates that in the case of using 3 shackles in the joint, the frame load capacity is greater by as much as 70% than when using 2 shackles. A similar trend is observed during the later stage of frame height reduction, until a value of approx. $\Delta H = 300$ mm, but the differences in frame load capacity at 2 and 3 shackles are no longer as prominent. Great fluctuations in the support frame load capacity can also be seen, which are typical of the operation of a severely strained support. The high relation of the maximum yielding frame load capacity of $F_{N\max}$ = 847 kN to the maximum load capacity in a rigid state of $F_{\max}$ = 1069 kN, as follows:

$$F_3 = \frac{F_{N\max}}{F_{\max}} = 0.7923 \tag{2}$$

This indicates that the maximum frame load capacity is used, which is related primarily to the high strength of the steel used to form the ŁP10/V32/4/A support frame (S480W steel), to a very good extent. For the purposes of standard calculations and support selection, the F_3 value is conventionally adopted as 0.5544 [49]. It is also significant that during testing the frame joints did not exhibit a propensity for jamming, and after the tests the frames did not reveal any deformations of the sections and the shackles in the joint.

The charts depicted in Fig. 2c and 2d present support frame load capacity trend lines in the form of linear characteristics $F = f(\Delta H)$. Although both the characteristics demonstrate a clear increase in load capacity as the frame height is decreased during the test, it must however be stressed that the correlation with experimental data can vary. This is influenced by the nature of the dry friction itself in the support frame sliding joints as well as by many other factors resulting primarily from the pressure force of the sections in the joint and the varying section surface condition, where the surface condition depends on the rolling process employed in a steel mill. The determined linear trend characteristic $F = f(\Delta H)$, defined on the basis of high peaks of the frame load capacity during yielding, can also be used for numerical simulations when modelling support load capacity, though it should be noted that significant differences may occur compared to actual support operation. Under actual support frame operation conditions, the load is never symmetrical, whereas the joints do not operate simultaneously during the yield (similarly as in the test facility) and are under compound stress.

The sudden increase in support load capacity $F_{N\max}$ observed in Fig. 2c was most likely the result of a temporary shift from a state of friction at the V32 section contact point surfaces into a state where the section ends would push into one another. As a consequence of this situation, the temporary load capacity of the ŁP10/V32/4/A support formed from S480W steel ($F_{N\max}$ = 714 kN

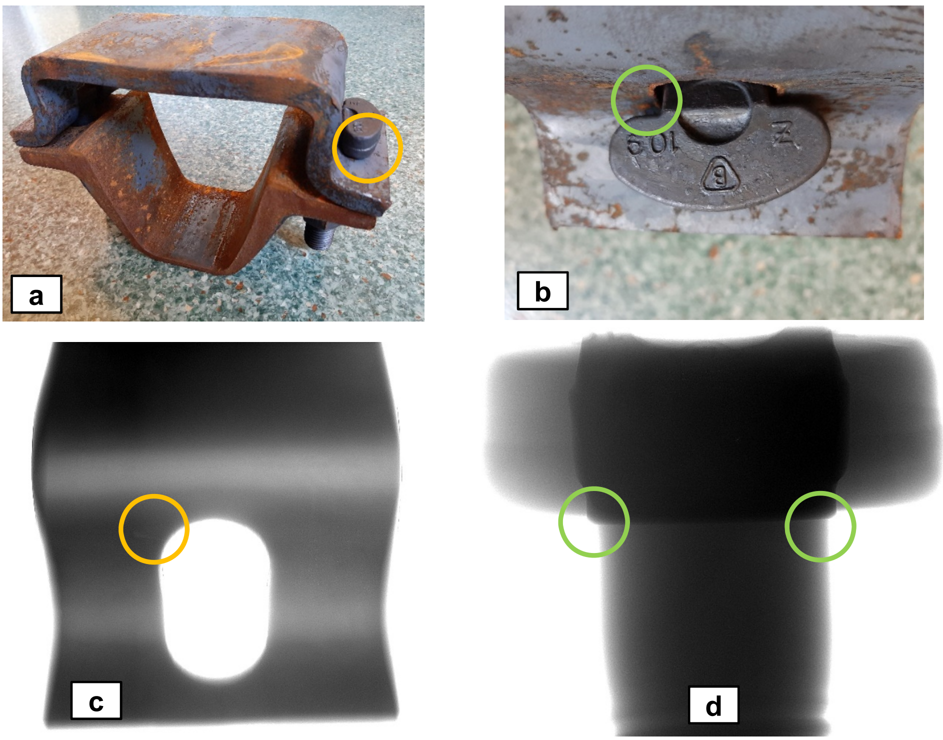

Fig. 3. Images of SD32/36W shackles after the tests: a and b – full shackle with marked areas of stress concentration; c – X-ray image of the upper clevis with a marked slightly indented area; d – X-ray image of a screw with no signs of damage
(Fig. 3c and 3d – Dominik Czachura, Smart Solutions, www.smart-solutions.pl)

with two shackles) was considerably higher compared to the load capacity of the same type of ŁP10/V32/4/A support but formed from S560W steel ($F_{N\max}$ = 587 kN with two shackles). Similar cases were also observed for other tests, including in the courses presented in Fig. 6c and 10c. It should however be noted that all these joints retained their ability for continued yielding during the tests. No significant deformations were found in the shackles used to couple the arches in the joints (Fig. 3a and 3b). This was confirmed by radiographic image analysis of the shackles, which also did not find any fractures in either the clevis or the screws, which can be seen in the X-ray images presented in Fig. 3c and 3d. A slight indentation was observed only around the opening in the clevis, at the contact point with the screw (Fig. 3b and 3c). The shackle screw, tightened with a torque of 500 Nm during the tests, remained undamaged, even in locations that are particularly susceptible to the occurrence of stress concentration [12,43] – between the screw head and shank.

Fig. 4 presents the test courses of ŁP10/V32/4/A support frames formed from S560W steel in rigid and yielding states, including the value of support work W.

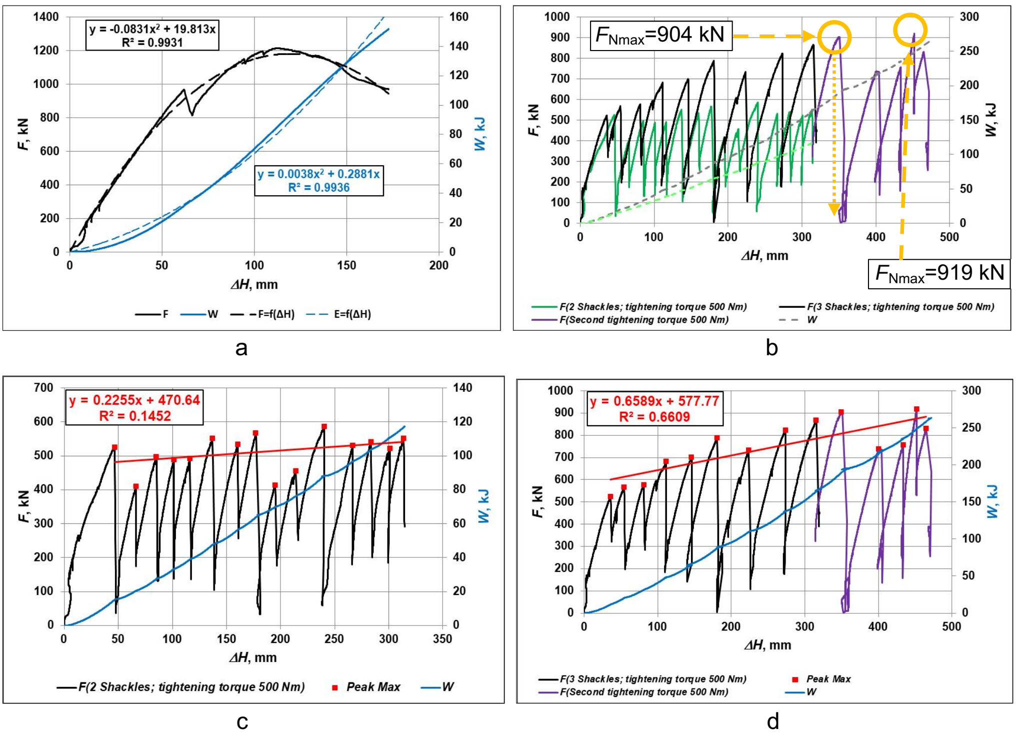

Fig. 4. Test courses of ŁP10/V32/4/A frames formed from S560W steel in various states:
a – rigid ($F_{\max}$ = 1214 kN); b – yielding: load capacity comparison for frames with 2 and 3 shackles;
c – yielding with 2 shackles ($F_{N\max}$ = 587 kN); d – yielding with 3 shackles ($F_{N\max}$ = 919 kN)

The maximum load capacity of the rigid ŁP10/V32/4/A support frame formed from S560W steel (Fig. 4a) was $F_{\max}$ = 1214 kN, while the support frame work at the end of the test was approx. W = 150 kJ. The maximum load capacity of the yielding ŁP10/V32/4/A support frame formed from

S560W steel (Fig. 4b, c and d) was $F_{N\max}$ = 587 kN with two shackles and $F_{N\max}$ = 919 kN with three shackles. The work value after a support frame height reduction by approx. ΔH = 300 mm was approx. W = 110 kJ (with two shackles) and approx. W = 150 kJ (with three shackles). The load capacity comparison chart for frames with 2 and 3 shackles demonstrates that in the case of using 3 shackles in the joint, the frame load capacity is greater by about 40% than when using 2 shackles. A similar trend is observed during the later stage of the 3-shackle frame height reduction, until a value of approx. ΔH = 300 mm, but with an increase in load capacity by as much as 55%. The relation of the maximum yielding frame load capacity of $F_{N\max}$ = 919 kN to the maximum load capacity in a rigid state of $F_{\max}$ = 1214 kN is high as well, amounting to:

$$F_3 = \frac{F_{N\max}}{F_{\max}} = 0.7570 \tag{3}$$

This also indicates that the maximum load capacity of the ŁP10/V32/4/A frame (formed from S560W steel) is used to a very good extent. During testing, the frame joints also did not exhibit a propensity for jamming, and after the tests were concluded the frames did not reveal any deformations of the sections or the shackles in the joint. The charts depicted in Fig. 4c and 4d present support frame load capacity trend lines in the form of linear characteristics $F = f(\Delta H)$. The 2-shackle ŁP10/V32/4/A frame load capacity characteristic exhibits weak correlation, and its trend shows only slight growth. On the other hand, the 3-shackle ŁP10/V32/4/A frame load capacity exhibits a clearly growing trend.

2.1.2. ŁP10/V36/4/A support frame test results

Fig. 5 presents the test courses of ŁP10/V36/4/A support frames formed from S480W steel in rigid and yielding states, including the value of support work W.

Fig. 5a presents two test courses for the ŁP10/V36/4/A support in a rigid state and typical top section damage in the form of twisting. The maximum loading force values obtained for both the tests were similar: $F_{\max}$ = 1175 kN (sample no. 1) and $F_{\max}$ = 1156 kN (sample no. 2). The work courses W = $f(\Delta H)$ were very similar until the point of local loss of stability in the support top section, which for both the tests occurred at a height reduction of $\Delta H \sim 80$ mm. However, the test conducted on sample no. 1 was interrupted immediately after the top section had undergone buckling (at F ~ 1000 kN and W ~ 120 kJ), whereas the test of sample no. 2 was continued until a height reduction of $\Delta H \sim 190$ mm was achieved. As can be observed in the chart, even after the local loss of top section stability (as a result of twisting), the support load capacity remained high, while the maximum support work reached a value of 180 kJ by the end of test no. 2.

The maximum load capacity of the yielding ŁP10/V36/4/A support frame (Fig. 5b, c and d) was $F_{N\max}$ = 518 kN with two shackles and $F_{N\max}$ = 883 kN with three shackles. The work value after a support frame height reduction by approx. ΔH = 300 mm was approx. W = 100 kJ (with two shackles) and approx. W = 150 kJ (with three shackles). The load capacity comparison chart for frames with 2 and 3 shackles demonstrates that in the case of using 3 shackles in the joint, the frame load capacity is greater by approx. 70% (throughout the course) than when using 2 shackles. The relation of the maximum yielding frame load capacity of $F_{N\max}$ = 883 kN to the maximum load capacity in a rigid state of $F_{\max}$ = 1175 kN is high as well, amounting to F_3 = 0.7515. During testing, the frame joints also did not exhibit a propensity for jamming, and after the tests were concluded the frames did not reveal any deformations of the sections or the shackles in the joint.

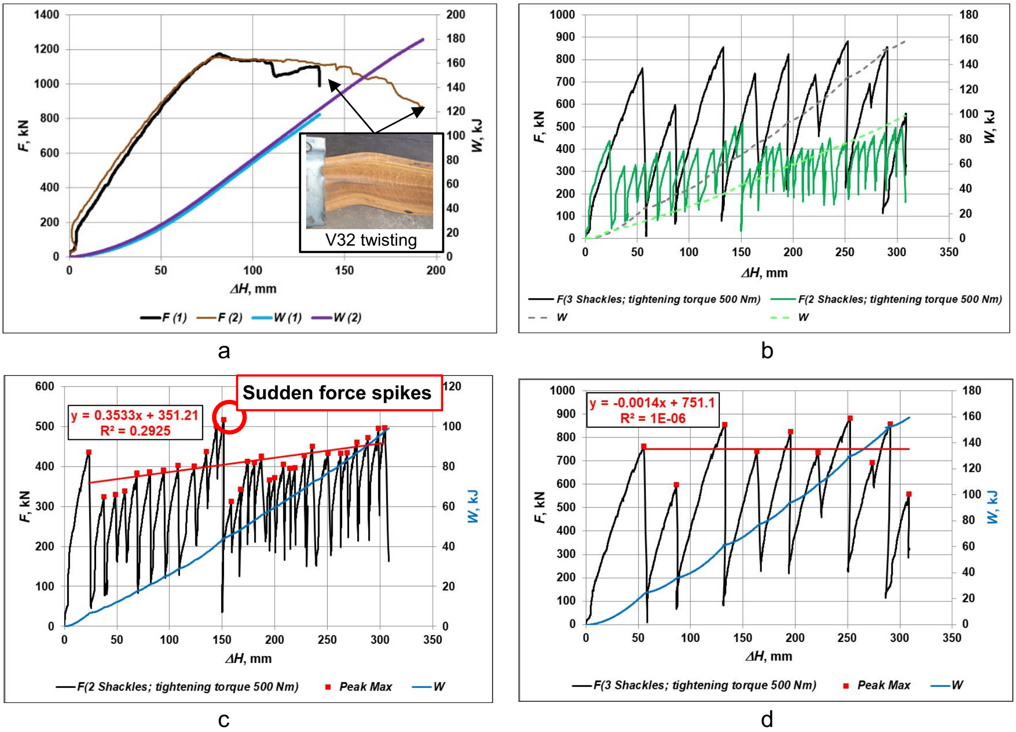

Fig. 5. Test courses of ŁP10/V36/4/A frames formed from S480W steel in various states:
a – rigid (F_{max} = 1175 kN (sample no. 1) and F_{max} = 1156 kN (sample no. 2));
b – yielding: load capacity comparison for frames with 2 and 3 shackles;
c – yielding with 2 shackles (F_{Nmax} = 518 kN); d – yielding with 3 shackles (F_{Nmax} = 883 kN)

2.1.3. ŁP10/V29/4/A support frame test results

Fig. 6 presents the test courses of ŁP10/V29/4/A support frames formed from S480W steel in rigid and yielding states, including the value of support work W.

The maximum load capacity of the rigid ŁP10/V29/4/A support frame formed from S480W steel (Fig. 6a) was F_{max} = 1023 kN, while the support frame work at the end of the test was approx. W = 120 kJ. The maximum load capacity of the yielding ŁP10/V29/4/A support frame (Fig. 6b, c and d) was F_{Nmax} = 494 kN with two shackles and F_{Nmax} = 770 kN with three shackles. The work value after a support frame height reduction by approx. ΔH = 300 mm was approx. W = 100 kJ (with two shackles) and approx. W = 125 kJ (with three shackles). The load capacity comparison chart for frames with 2 and 3 shackles demonstrates that in the case of using 3 shackles in the joint, at times the frame load capacity is greater by more than 90%. The relation of the maximum yielding frame load capacity of F_{Nmax} = 770 kN to the maximum load capacity in a rigid state of F_{max} = 1023 kN is high, amounting to F_3 = 0.7527. During testing, the frame joints did not exhibit a propensity for jamming, and after the tests were concluded the frames did not reveal any deformations of the sections or the shackles in the joint.

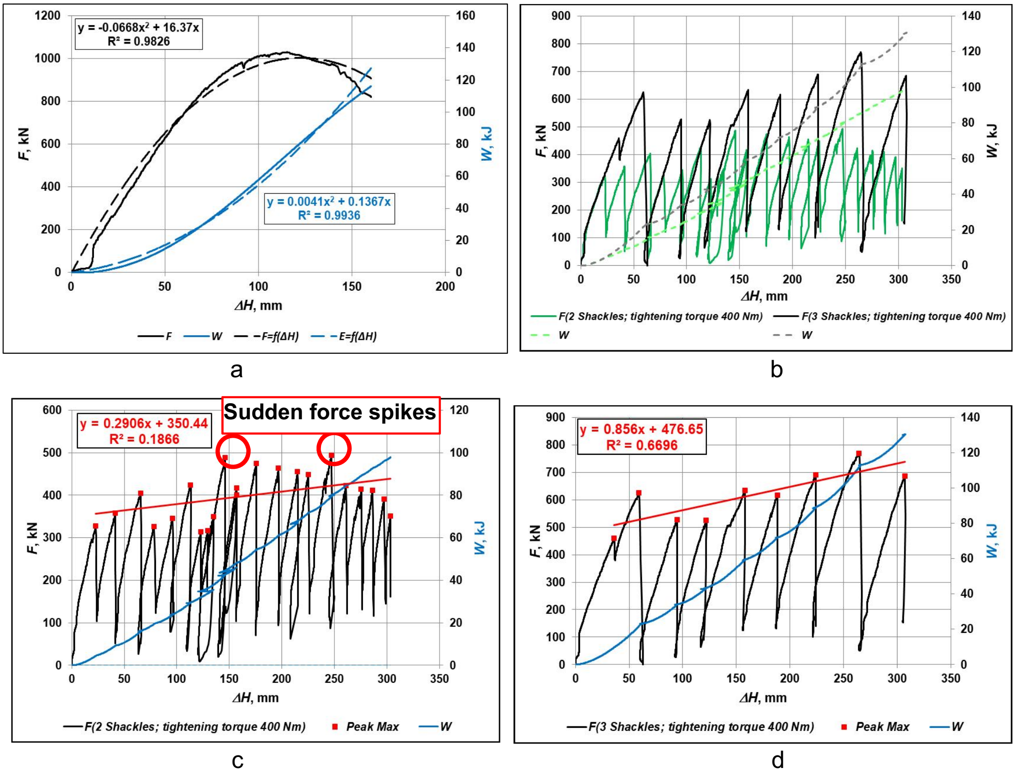

Fig. 6. Test courses of ŁP10/V29/4/A frames formed from S480W steel in various states:
a – rigid (F_{max} = 1023 kN); b – yielding: load capacity comparison for frames with 2 and 3 shackles;
c – yielding with 2 shackles (F_{Nmax} = 494 kN); d – yielding with 3 shackles (F_{Nmax} = 770 kN)

2.2. Tests of arch acceleration in sliding joints and joint heating temperature during yielding

A view of the test facility during the performance of top section acceleration and joint heating tests is presented in Fig. 7.

The acceleration courses for a top section in a joint with a side section of the yielding ŁP10/V32/4/A frame formed from S560W steel with 3 shackles are presented in Fig. 8.

Fig. 9 presents the registered mechanical sparking occurring during yielding in the joint, the acceleration course of which is depicted in Fig. 4b.

A typical acceleration course for a top section in a joint with a side section of the yielding ŁP10/V36/4/A frame formed from S480W steel with 2 shackles is presented in Fig. 10a. Fig. 10b on the other hand presents the temperature distribution in this joint during the yield Y, as a function of time (Y = 60 mm, a_{max} = 919 m/s^2, F_{Nmax} = 518 kN).

Fig. 11 presents pictures of the joint before and after yielding as well as thermal images indicating the location of sparking along with temporary and maximum temperature values.

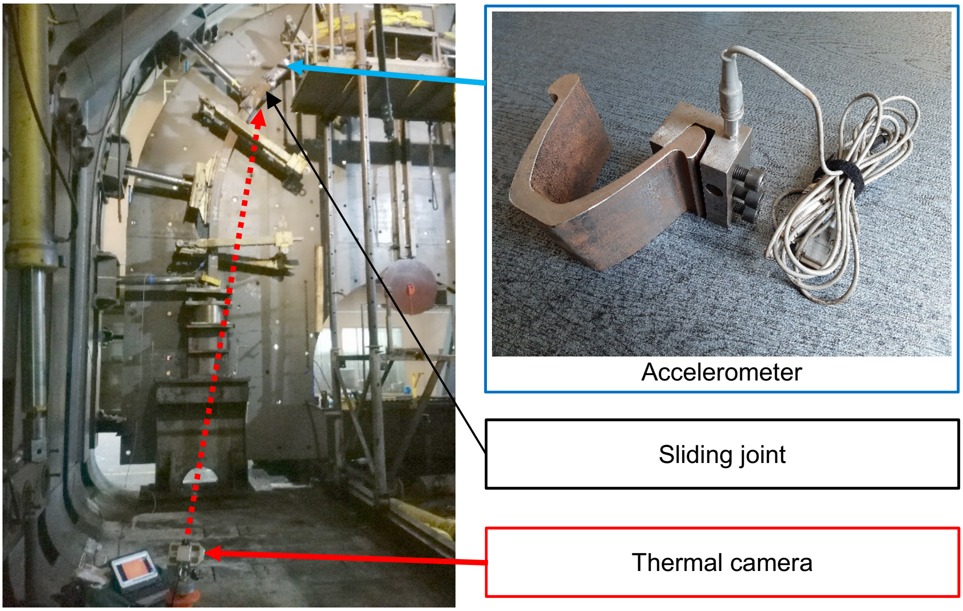

Fig. 7. Test facility during top section acceleration and joint heating tests

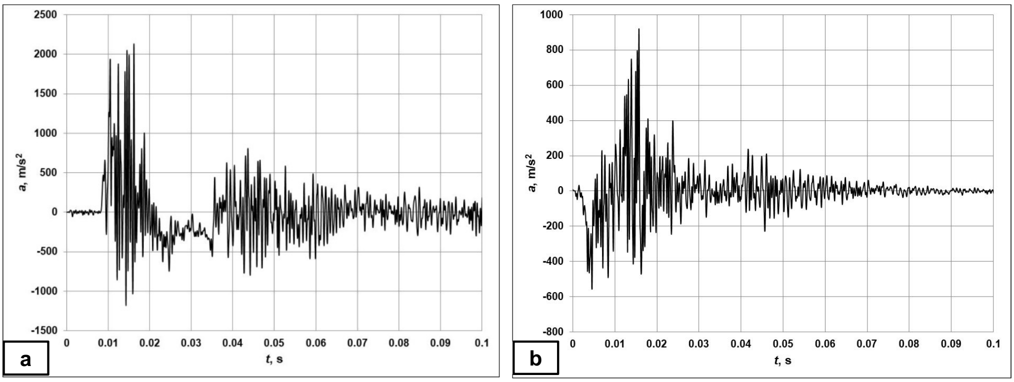

Fig. 8. Top section acceleration courses during a yield in a joint with a side section (3 shackles in the joint): a – a_{max} = 2125 m/s^2 at a yield of 130 mm and initial force of 904 kN; b – a_{max} = 920 m/s^2 at a yield of 30 mm and force of 738 kN

The maximum temperature was registered at the upper shackle in the joint and amounted to approx. T_{max} = 100°C, while at the lower shackle it was T_{max} = 46°C. Both the temperatures are lower than the criterion value of T = 150°C defined in the requirements of standard EN ISO 80079-36:2016 harmonised with the ATEX directive concerning group I non-electrical equipment intended for use under the conditions of explosive atmospheres and the presence of coal dust layers.

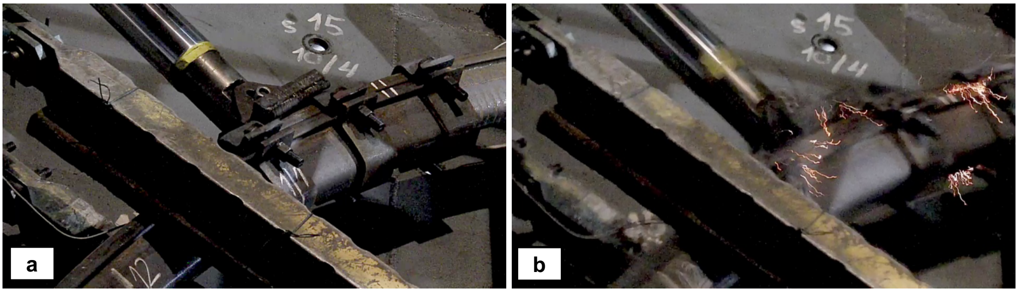

Fig. 9. Registered mechanical sparking in a joint during a 130 mm long yield at a section acceleration of a_{max} = 2125 m/s^2; a – before the yield; b – during the yield

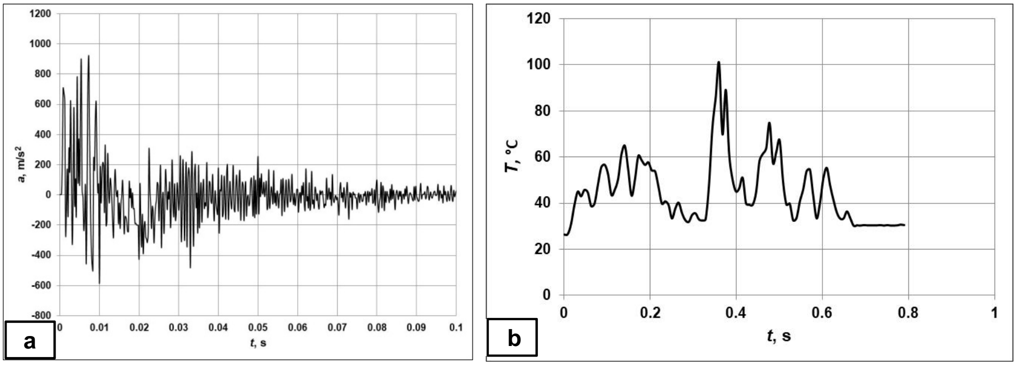

Fig. 10. Typical course of top section acceleration in a joint (a) and temperature distribution in the joint as a function of time (b)

Tests of the same type of ŁP10/V36/4/A frame formed from S480W steel in a yielding state with 3 shackles found (Fig. 12) that the registered maximum temperature was T_{max} = 46°C, therefore considerably lower than during the operation of the same support type with 2 shackles. This is related to the beneficial influence of the third, middle shackle, which contributes to the equalisation of pressures in the joint and the decrease in contact point pressures in the terminal shackle areas: the upper and lower shackle. No mechanical sparking was observed in the middle shackle area.

2.3. Results of sliding joint tests under dynamic loading

The main goal of the sliding joint tests under dynamic loading was to determine the influence of the third (middle) shackle on the joint load capacity and on limiting the joint yield in such a way so as to inhibit it during the test to prevent a total yield of the sections in the joint.

The principle of the V32 sliding joint dynamic resistance test is the free fall of a drop mass (ram) m_1 = 4000 kg from a height h onto a cross-bar with a mass m_2 = 3300 kg, which applies static loading to the joint mounted in the test facility. The height h was progressively increased until total

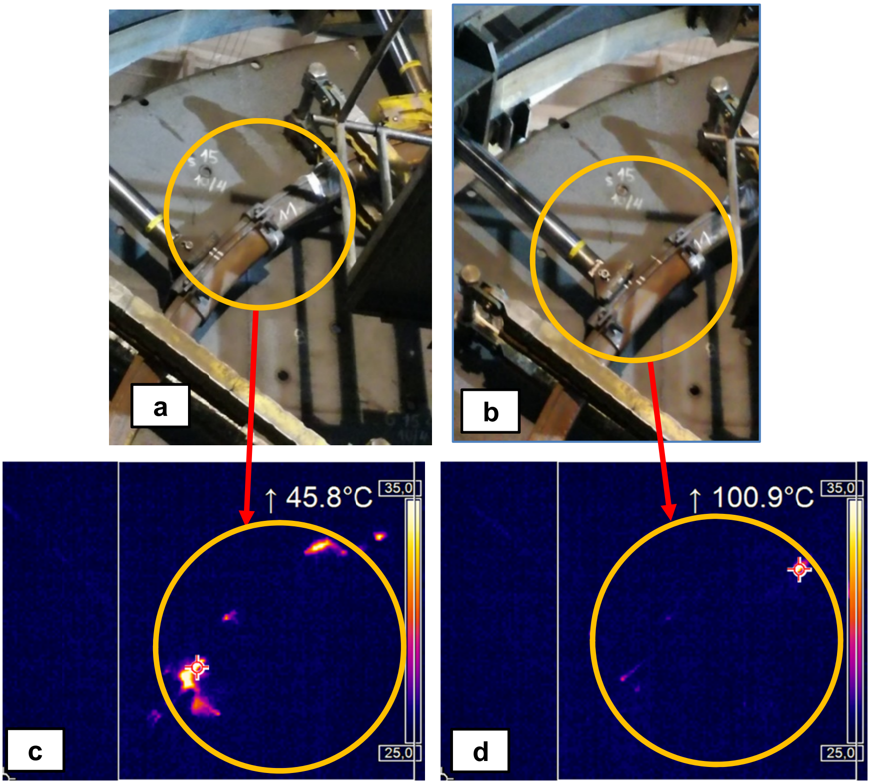

Fig. 11. Temperature distributions in a joint during yielding (Y = 60 mm, a_{max} = 919 m/s^2, F_{Nmax} = 518 kN) for a yielding ŁP10/V36/4/A frame formed from S480W steel with 2 shackles

sliding joint yield was achieved. The drop height varied within the range of h = 5-70 cm, which corresponds to an impact velocity range of v = 1-3.7 m/s, calculated using the following formula:

$$v = \sqrt{2gh}, \text{m/s} \tag{4}$$

where: g – gravitational acceleration.

15 tests were performed in total, using a ram with a mass of m_1 = 4000 kg applied against joints constructed from V32 sections with 2 and 3 SD32 shackles whose screws were tightened with a nominal torque of M_d = 450 Nm. The tested sliding joints had a base (nominal) yield load of F_s = 410 kN, determined under static loading according to standard PN-G-15533:1997 [30]. In order to inspect the load capacity and yield of a joint with 3 shackles at an impact mass similar to its static load capacity, a single test was performed using a ram with a mass m_1 = 20,000 kg dropped onto a cross-bar with a mass m_2 = 3300 kg from a height h = 5 cm.

Fig. 13 presents a diagram and a picture of the test facility with a 4.8 m tall sliding joint constructed from two V32 sections coupled using two or three (after adding a middle shackle) SD32 shackles. The axial force exerted on the joint during the free fall of mass m_1 was measured

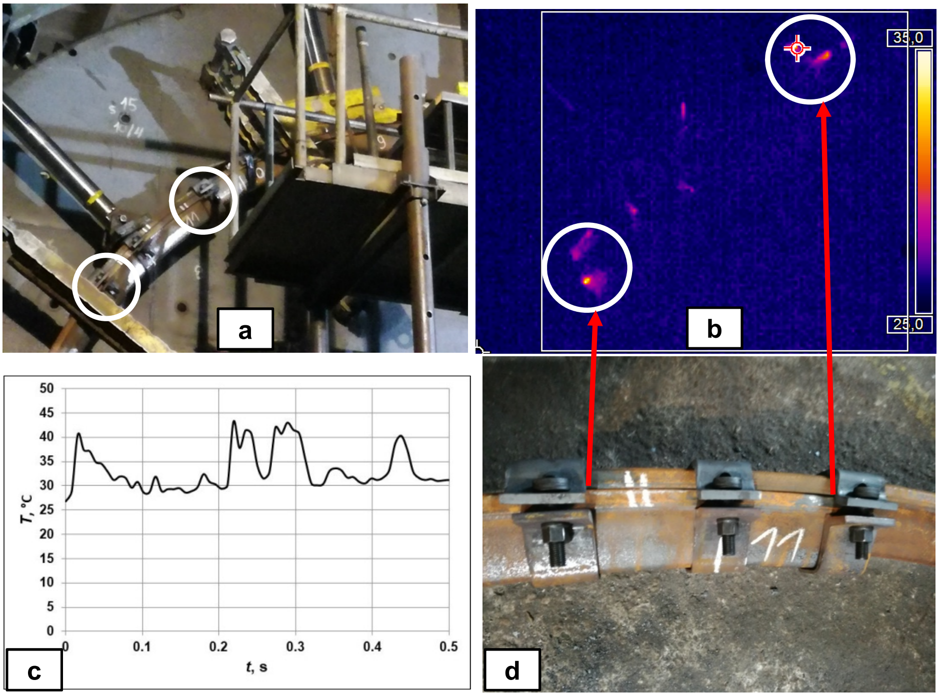

Fig. 12. Tests of yielding ŁP10/V36/4/A frames formed from S480W steel with 3 shackles:
a – picture of a sliding joint with 3 shackles; b – sliding joint thermal image; c – temperature distribution in the joint as a function of time; d – post-test picture of a sliding joint

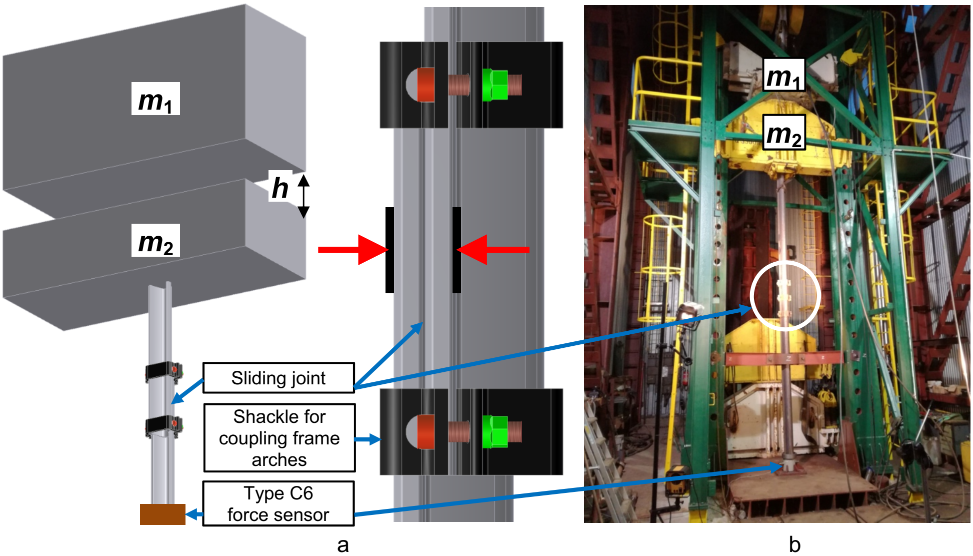

Fig. 13. Diagram (a) and picture (b) of the facility for sliding joint tests under dynamic loading

during the test by means of a class 0.5 (5 MN measuring range, f_s = 9600 Hz) C6 strain gauge force sensor. The joint yield Y was measured before and after the test using a gauge. In order to analyse [50] the phenomena occurring during the studies, the tests were recorded using two independent high-speed video cameras (600 and1000 frames per second).

Typical courses of force F_d as a function of time t obtained during testing of joints with 2 shackles are presented in Fig. 14, and during testing of joints with 3 shackles in Fig. 15.

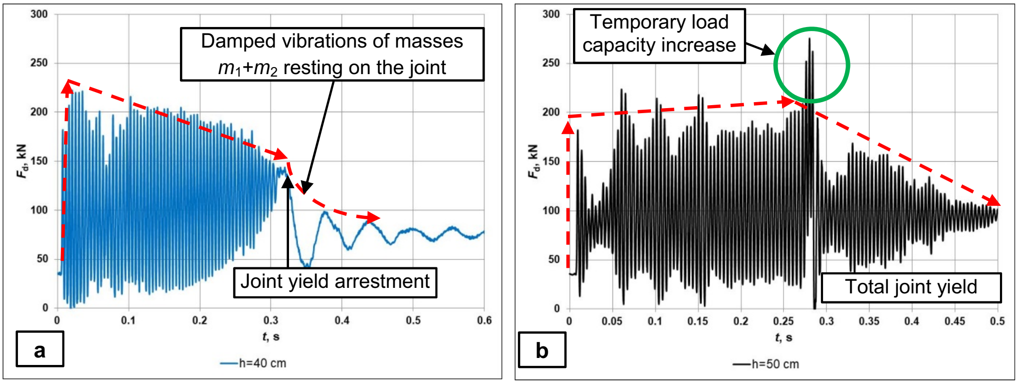

Fig. 14. Courses of load F_d as a function of time t under dynamic loading of a joint (2 shackles) at the following parameters: h = 40 cm, m_1 = 4000 kg, v = 2.8 m/s, $F_{d\max}$ = 223 kN, Y = 261 mm (a), and h = 50 cm, m_1 = 4000 kg, v = 3.1 m/s, $F_{d\max}$ = 276 kN, Y > 420 mm (b)

The temporary increase in load capacity depicted in Fig. 14b might have been the result of the formation of a splinter on the section surfaces in the joint, though its influence on the increase in joint load capacity was not great enough to inhibit its yield. The joint underwent total yield.

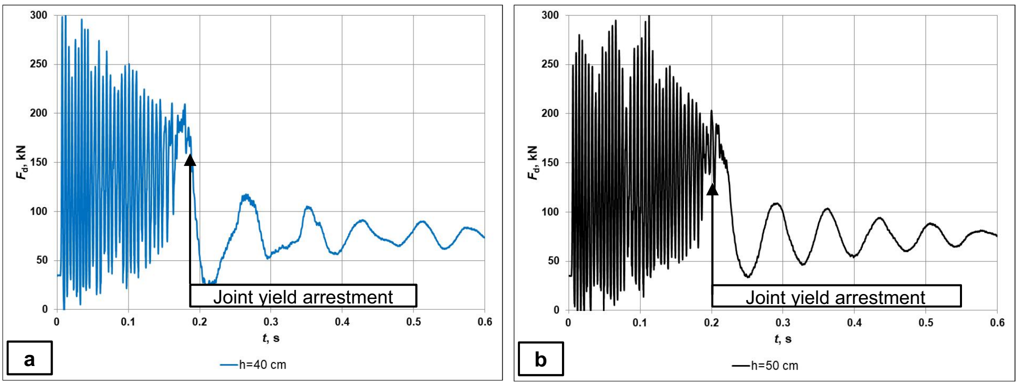

Fig. 15. Courses of load F_d as a function of time t under dynamic loading of a joint (3 shackles) at the following parameters: h = 40 cm, m_1 = 4000 kg, v = 2.8 m/s, $F_{d\max}$ = 310 kN, Y = 141 mm (a), and h = 50 cm, m_1 = 4000 kg, v = 3.1 m/s, $F_{d\max}$ = 301 kN, Y = 196 mm (b)

The comparative test results of sliding joints constructed from V32 sections with 2 and 3 shackles demonstrate that the sliding joint load capacity decreases and its yield is extended together with the increase in impact velocity *v*. Total joint yield occurs after a specific impact velocity is exceeded, which transpired in the case of a joint with 2 shackles at a velocity of $v = 3.1$ m/s ($h = 0.5$ m). Similar phenomena were observed during tests of sliding joints constructed from V29 sections with 2 shackles [18]. In the case of a joint with 3 shackles, the joint was halted at a ram drop height range of h = 0-0.7 m, and the maximum yield was $Y = 196$ mm (Fig. 15b). According to standard PN-G-15533:1997, the criterion value used to determine whether a test outcome is positive is the drop height $h = 0.7$ m during the fall of a mass $m_1 = 4000$ kg. Therefore, the assessment of the V32 joint with 2 shackles in reference to the standard requirements is negative, whereas the assessment of the V32 joint with 3 shackles is positive. The courses presented in Fig. 14 and 15 demonstrate that the arrestment time for the joint with 3 shackles is shorter as well, which in practice limits the further acceleration capability of rocks that exert dynamic load on the working.

The course of the non-standard test using a ram with a mass $m_1 = 20{,}000$ kg applied against a joint constructed from V32 sections coupled with 3 shackles as well as pictures of the joint before and after the test are presented in Fig. 16.

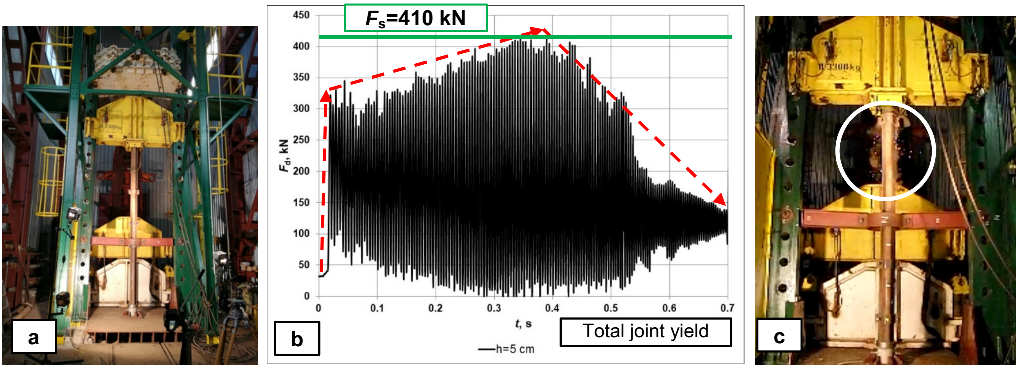

Fig. 16. Course of load F_d as a function of time *t* under dynamic loading of a joint (3 shackles): a – pre-test joint; b – test course at the following parameters: $h = 5$ cm, $m_1 = 20{,}000$ kg, $v = 1$ m/s, $F_{d\max} = 415$ kN, $Y > 1035$ mm; c – post-test joint with visible mechanical sparking in the upper shackle area

Previous tests performed according to standard PN-G-15533:1997 determined that the nominal static joint load capacity was $F_s = 410$ kN. Before the bench test was carried out (Fig. 16a), another examination revealed that placing a total mass of $m = m_1 + m_2 = 23{,}300$ kg, exerting a static load on the joint, did not result in yielding. However, a test at $h = 5$ cm ($v = 1$ m/s) resulted in total joint yield $Y > 1035$ mm that did not manage to inhibit the accelerating mass *m* (Fig. 16b). This is confirmed by the test course, which first presents a systematic increase in joint load capacity until a value of $F_{d\max} = 415$ kN (close to the nominal static joint load capacity of $F_s = 410$ kN), whereas, subsequently, together with increasing joint acceleration, the dynamic load capacity exhibited a sharp decrease to a value of approx. 140 kN (at the final stage of the yield). The possibility of the occurrence of such a great decrease in joint load capacity, by as much as

66% compared to the static load capacity, must be taken into consideration when designing support systems for rock burst hazard conditions. However, load capacity determination at impact velocities lower than 1 m/s requires further testing, which due to its specifics – very high impact mass and energy – is hazardous to both the test facility and the measuring apparatus.

3. Summary and discussion

The test results of size-10 support frames of the following types: ŁP10/V36/4/A, ŁP10/V32/4/A and ŁP10/V29/4/A formed from S480W and S560W steel demonstrate that:

- the ŁP10/V32/4/A support frame formed from S560W steel exhibited the highest load capacity in a rigid state, amounting to F_{max} = 1214 kN. Tests have shown that it is possible to determine the rigid support frame load capacity characteristic $F = f(\Delta H)$ using a mathematical function, and the correlation between it and the experimental course is very high. A given characteristic $F = f(\Delta H)$ in the form of a square function can therefore be used for numerical simulations when modelling support load capacity.
- the ŁP10/V32/4/A support frame formed from S560W steel with 3 shackles (M_d = 500 Nm) exhibited the highest load capacity in a yielding state, amounting to $F_{N\max}$ = 919 kN. The load capacity comparison chart for frames with 2 and 3 shackles demonstrates that in the case of using 3 shackles in the joint, the frame load capacity is greater by about 40% than when using 2 shackles. A similar trend is observed during the later stage of the 3-shackle frame height reduction, until a value of approx. ΔH = 300 mm, but with an increase in load capacity by as much as 55%. At the same time, the relation of the maximum yielding frame load capacity of $F_{N\max}$ = 919 kN to the maximum load capacity in a rigid state of F_{max} = 1214 kN is high as well, at F_3 = 0.7570, which indicates that the maximum load capacity of the ŁP10/V32/4/A frame (formed from S560W steel) is used to a very good extent. During testing, the frame joints did not exhibit a propensity for jamming, and after the tests were concluded the frames did not reveal any deformations of the sections and the shackles in the joint.
- The maximum top section acceleration values in the joints exceeded an amplitude of a = 2000 m/s^2. Though such a high acceleration has no influence on the sliding joint operation, it may have a negative influence on its interaction with rock bolts, which are often utilised in the field as reinforcement elements for the support frame top section.
- Thermal imaging did not reveal any surface heating during the joint yield that would be hazardous from the perspective of the ATEX directive [51-53]. The measured temperature reached a value of approx. T_{max} = 100°C during testing of the yielding ŁP10/V36/4/A frame formed from S480W steel with 2 shackles. Tests of the same frame type but with 3 shackles found that the registered maximum temperature was T_{max} = 46°C, therefore considerably lower than during the operation of the same support type but with 2 shackles. This demonstrates the beneficial influence of the third, middle shackle, which contributes to the equalisation of pressures in the joint and the decrease in contact point pressures in the terminal shackle areas: the upper and lower shackle.

Comparative tests of sliding joints constructed from V32 sections with 2 and 3 shackles demonstrate that the sliding joint load capacity decreases and its yield is extended together with an increase in impact velocity v. Total joint yield occurs after a specific impact velocity is exceeded, which transpired in the case of a joint with 2 shackles at a velocity of v = 3.1 m/s (h = 0.5 m). According to standard PN-G-15533:1997, the criterion value used to determine whether a test outcome is positive is the drop height h = 0.7 m during the fall of a mass m_1 = 4000 kg. Thus, the assessment of the V32 joint with 2 shackles in reference to the standard requirements is negative, whereas the assessment of the V32 joint with 3 shackles is positive. The results of a single test of a sliding joint constructed from V32 sections with 3 shackles using a ram mass m_1 = 20,000 kg found that performing the test at h = 5 cm (v = 1 m/s) resulted in a total joint yield Y > 1035 mm that did not manage to inhibit the accelerating mass. The reason for this was a large decrease in joint load capacity, by as much as 66% compared to the static load capacity. However, load capacity determination at impact velocities lower than 1 m/s requires further testing, which, due to its specifics (i.e. very high impact mass and energy), is hazardous to both the test facility and the measuring apparatus. Yet this phenomenon of joint load capacity decrease under dynamic loading should be taken into consideration when designing support systems for rock burst hazard conditions, as it may hold great significance for the safety of personnel as well as the support itself.

4. Conclusions

Based on the support frame and sliding joint tests performed, it can be concluded that adding a third (middle) shackle to the sliding joint considerably increases its static and dynamic load capacities, while increasing the shackle screw torque to a value of M_d = 500 Nm amplifies the effect even further. This can be seen particularly clearly during support operation at the first stage of its height reduction, which has been conventionally defined at a range of ΔH = 0-100 mm. Utilising the third shackle in the joint also considerably limits the yield value, which in extreme cases could prevent the support from losing stability and blocking the working during the occurrence of roof rock fall or rock burst. Using a high-strength grade of steel such as S480W, and particularly S560W, considerably increases the support load capacity in a rigid state and protects it from plastic arch deformation that could result in joint jamming and, therefore, in support yield loss. Thanks to this, the k_3 factor that indicates the degree to which the maximum frame load capacity is utilised can reach a value close to 0.8, which greatly exceeds current standards (k_3 = 0.5544).

The determined temperature distribution in the joint and the mechanical sparking location distribution indicate that the greatest temperatures occur at the ends of the joint (in the areas of the upper and lower shackles), regardless of whether the joint has 2 or 3 shackles. The use of the third, middle shackle in the joint significantly decreases this temperature, which is most likely the result of the equalisation of section contact pressure forces along its length, as well as the simultaneous decrease in contact pressure force in the upper and lower shackles.

The results of top section acceleration tests indicate that the top section acceleration values during yielding exceed 2000 m/s^2 (200g). This may be the reason why rock bolts coupled directly with the support frame or indirectly via rigid joists tend to sustain damage. The accumulated elastic strain energy in the deforming support arches undergoes sudden dissipation in the joint during its yielding when load is exerted on the support. This phenomenon is also accompanied by heat release and mechanical sparking. To secure the rock bolts against dynamic loading generated by the yield in the frames, it is recommended that they not be coupled with the frames directly, or for their coupling, e.g. via a short joist [24], to have yielding properties. Rock mass bolting between the support frames can also be carried out. Such a support system is characteristic of mixed supports utilising arches and rock bolts, and it is the best way of combining the properties of a rigid rock bolt support with those of a yielding steel arch support.

References

[1] T. Majcherczyk, Z. Niedbalski, P. Małkowski, Ł. Bednarek, Analysis of yielding steel arch support with rock bolts in mine roadways stability aspect. Archives of Mining Sciences **59** (3), 641-654, (2014), DOI: 10.2478/amsc-2014-0045.

[2] T. Majcherczyk, S. Prusek, P. Małkowski, Z. Niedbalsk, M. Rotkegel, Ł. Szot, Stalowa obudowa podporowa podatna wyrobisk korytarzowych w kopalniach Jastrzębskiej Spółki Węglowej SA: stan obecny i kierunki rozwoju. [Yielding steel arch support in the gallery workings of Jastrzębska Spółka Węglowa SA mines: present state and directions for development]. Główny Instytut Górnictwa, Katowice, Poland, (2016).

[3] A.K. Verma, T.N. Singh, Influence of Young's Modulus and Poisson's Ratio on the Displacement Around a Circular Tunnel. In Earth System Processes and Disaster Management , 181-201, Springer, Berlin, Heidelberg, (2013), https://doi.org/10.1007/978-3-642-28845-6_13.

[4] G. Bräuner, Gebirgsdruck und Gebirgsschläge: Fragen der Standsicherheit von Grubenbauen. [Rock pressure and rock burst: questions of the stability of mine support] 2. Auflage, Essen: Verlag Glückauf, (1991).

[5] J. Dubiński, W. Konopko, Tąpania: ocena, prognoza, zwalczanie [Tremors: evaluation, forecast, elimination]. Główny Instytut Górnictwa, Katowice (in Polish), (2000).

[6] J. Dubiński, G. Mutke, (Characteristics of mining tremors within the near-wave field zone. In Induced Seismic Events, 249-261, Birkhäuser Basel, 1996), DOI: 10.1007/978-3-0348-9204-9_4.

[7] W. Müller, Numerical simulation of rock bursts. Mining science and technology **12** (1), 27-42 (1991).

[8] J. Ptáček, P. Koníček, J. Holečko, A. Przeczek, P. Waclawik, Z. Pavelek, M. Macura, V. Kajzar, R. Kukutsch, Rockbursts in Ostrava Karviná Coalfield. Ústav geoniky AV ČR, v.v.i., Ostrava, (2017).

[9] M. Chudek, Obudowa wyrobisk górniczych. Część 1. Obudowa wyrobisk korytarzowych i komorowych. [Mine working support. Part 1. Gallery and chamber working support]. Wydawnictwo „Śląsk". Poland (1986).

[10] M. Grodzicki, M. Rotkegel, The concept of modification and analysis of the strength of steel roadway supports for coal mines in the Soma Basin in Turkey. Studia Geotechnica et Mechanica **40** (1), 38-45 (2018).

[11] P. Horyl, R. Šňupárek, Behaviour of steel arch supports under dynamic effects of rockbursts. Mining Technology **116** (3), 119-128 (2007).

[12] P. Horyl, R. Šňupárek R., P. Marsalek, Behaviour of frictional joints in steel arch yielding supports. Archives of Mining Sciences **59** (3), 723-734 (2014).

[13] P. Horyl, R. Šňupárek R., P. Marsalek, K. Pacześniowski, Simulation of laboratory test of steel arch support. Archives of Mining Sciences **62** (1), 163-176 (2017).

[14] O. Jacobi, Praxis der Gebirgsbeherrschung. [Roof control practice]. 2. Auflage, Essen, Verlag Glückauf GmbH, Germany, (1981).

[15] S.G. Jukes, F.P. Hassani, B.N. Whittaker, Characteristics of steel arch support systems for mine roadways. Part. 1. Modelling theory, instrumentation and preliminary results. Mining Science and Technology **1** (1), 43-58 (1983).

[16] H. Kang, Support technologies for deep and complex roadways in underground coal mines: a review. International Journal of Coal Science & Technology **1** (3), 261-277. DOI: 10.1007/s40789-014-0043-0, (2014).

[17] R. Podjadtke, H. Witthaus, J. Breedlove, Development in steel roadway support-a track record. In The 27th International Conference on Ground Control in Mining, Morgantown, West Virginia, 358-365, (2009, July).

[18] A. Pytlik, Tests of steel arch and rock bolt support resistance to static and dynamic loading induced by suspended monorail transportation. Studia Geotechnica et Mechanica **41** (2), 81-92 (2019).

[19] X. Sun, L. Wang, Y. Lu, B. Jiang, Z. Li, J. Zhang, A yielding bolt - grouting support design for a soft-rock roadway under high stress: a case study of the Yuandian No. 2 coal mine in China. Journal of the Southern African Institute of Mining and Metallurgy **118** (1), 71-82 (2018).

[20] M. Turek, Podstawy podziemnej eksploatacji pokładów węgla kamiennego. [The basics of underground hard coal deposit extraction]. Główny Instytut Górnictwa, Katowice, (2010).

[21] Y. Zhao, N. Liu, X. Zheng, N. Zhang, Mechanical model for controlling floor heave in deep roadways with U-shaped steel closed support. International Journal of Mining Science and Technology **25** (5), 713-720 (2015).

[22] A. Nierobisz, Obudowa podporowo-kotwiowa dla rozcinek rozruchowych ścian - przykłady zastosowań. [Mixed support system for longwall cross-cuts – examples of application]. Nowoczesne technologie górnicze. Problemy utrzymania wyrobisk korytarzowych. Politechnika Śląska w Gliwicach. Stowarzyszenie Inżynierów i Techników Górnictwa, Gliwice, Ustroń 20-21 April, 131-155 (2006).

[23] A. Pytlik, Stanowisko i metodyka badań obudowy podporowo-kotwiowej w skali naturalnej. [Full-scale mixed support test stand and methodology]. Przegląd Górniczy **8**, 18-23 (2017).

[24] A. Pytlik, Comparative Bench Testing of Steel Arch Support Systems with and Without Rock Bolt Reinforcements. Archives of Mining Sciences **64 (**4), 747-764 (2019).

[25] M. Turek (Ed.), Bezpieczeństwo obudowy podporowo-kotwiowej w warunkach występowania wstrząsów górotworu. [Mixed support safety under the conditions of rock mass tremor occurrence]. Główny Instytut Górnictwa, Katowice, (2012).

[26] M. Turek, S. Prusek, W. Masny, Obudowa podporowo-kotwiowa w kopalniach węgla kamiennego. [Mixed support in hard coal mines]. Główny Instytut Górnictwa, Katowice, (2015).

[27] M. Cała, J. Flisiak, A. Tajduś, Mechanizm współpracy kotwi z górotworem o zróżnicowanej budowie. [The interaction between a rock bolt and a rock mass with varied structure]. Biblioteka Szkoły Eksploatacji Podziemnej. Seria z Lampką Górniczą 8. Kraków (in Polish), (2001).

[28] PN-G-15022:2018-11. Obudowa wyrobisk górniczych. Odrzwia podatne z kształtowników korytkowych. Wymagania wytrzymałościowe i badania. [Mine working support. Yielding frames constructed from channel sections. Strength requirements and testing].

[29] PN-G-15011:2011. Obudowa chodników odrzwiami podatnymi z kształtowników korytkowych. Strzemiona. [Road support by means of yielding frame sets constructed from channel sections. Shackles].

[30] PN-G-15533:1997. Górnicza obudowa indywidualna. Stojaki cierne. Wymagania i badania. [Single prop support. Friction props. Requirements and testing].

[31] PN-H-84042:2009/Az1:2012. Stale mikrostopowe na kształtowniki i akcesoria górnicze. [Micro-alloyed steel for mine equipment and sections].

[32] PN-H-93441-1:2013-12. Kształtowniki stalowe walcowane na gorąco dla górnictwa. Wymagania ogólne i badania. [Hot-rolled steel sections for mining. General requirements and testing].

[33] PN-H-93441-3:2004. Kształtowniki stalowe walcowane na gorąco dla górnictwa. Kształtowniki typu V. Wymiary. [Hot-rolled steel sections for mining. V sections. Dimensions].

[34] A. Pytlik, K. Stoiński, Odporność dynamiczna stalowych obudów odrzwiowych w świetle dotychczasowych badań. [Steel arch support dynamic resistance in the light of current studies], in: K. Rułka (Ed.), Stalowe obudowy odrzwiowe. Nowe rozwiązania konstrukcyjne i metody projektowania. [Steel frame support. New structural solutions and design methods], Główny Instytut Górnictwa, Katowice, 61-90 (2006).

[35] A. Pytlik, S. Prusek, W. Masny, A methodology for laboratory testing of rockbolts used in underground mines under dynamic loading conditions. SAIMM Journal of The Southern African Institute of Mining and Metallurgy **116**(12), 1101-1110 (2016).

[36] DIN 21530-4:2016-09. Mine support – Part 4: Testing.

[37] PN-G-15021:2019-05. Obudowa wyrobisk górniczych. Odrzwia podatne z kształtowników korytkowych. Odrzwia łukowe podatne ŁP z kształtowników typu V. [Mine working support. Yielding frames constructed from channel sections. ŁP yielding arch frames constructed from V-type sections].

[38] UNE 22725:2007. Sliding steel profiles for roof support.

[39] J. Brodny, Identyfikacja parametrów pracy złącza ciernego stosowanego w górniczej obudowie podatnej wyrobisk korytarzowych. [Operational parameter identification of sliding joints employed in yielding gallery support systems]. Wydawnictwo Politechniki Śląskiej, Gliwice, (2012).

[40] J. Brodny, Analysis of operation of new construction of the frictional joint with the resistance wedge. Archives of Mining Sciences **57** (1), 209-227 (2012).

[41] J. Brodny, Analysis of operation of arch frictional joint loaded with the impact of freely falling mass. Studia Geotechnica et Mechanica **35** (1), 59-71 (2013).

[42] P. Horyl, R. Snuparek, M. Hlavackova, Loading capacity of yielding connections used in steel arch roadway supports. In Proceedings of the Seventh International Symposium on Ground Support in Mining and Underground Construction, 461-470, Australian Centre for Geomechanics, (2013, May).

[43] P. Maršálek, P. Horyl, Modelling of bolted connection with flexible yokes used in mining industry. In AIP Conference Proceedings (**1863,** 1, 340008). AIP Publishing LLC, (2017, July).

[44] A. Pytlik, PhD thesis, Wpływ zginania na pracę ciernych złączy łukowych odrzwi ŁP przy obciążeniach statycznych i dynamicznych. [The influence of bending on yielding arch frame sliding joint operation under static and dynamic loads]. Główny Instytut Górnictwa, Katowice, (2001).

[45] A. Pytlik, Charakterystyka pracy ciernych złączy odrzwi obudowy ŁP przy obciążeniach statycznych i dynamicznych. [Operational characteristics of yielding arch frame support sliding joints under static and dynamic loads]. Prace Naukowe GIG **42**, Główny Instytut Górnictwa, Katowice, (2002).

[46] M. Rotkegel, ŁPW steel arch support – designing and test results. Journal of Sustainable Mining **12** (1), 34-40 (2013).

[47] PN-EN ISO 80079-36:2016-07 - Explosive atmospheres – Part 36: Non-electrical equipment for explosive atmospheres – Basic method and requirements.

[48] Europejskie Technologie Górnicze Ltd., https://czh.pl/spolka/europejskie-technologie-gornicze/: accessed: 09.03.2020.

[49] K. Rułka (Ed.), Uproszczone zasady doboru obudowy odrzwiowej wyrobisk korytarzowych w zakładach górniczych wydobywających węgiel kamienny. [Simplified gallery working frame support selection principles for mining plants extracting hard coal]. Główny Instytut Górnictwa, Zakład Technologii Eksploatacji i Obudów Górniczych, Katowice, (2001).

[50] M. Michalak, K. Nurzyńska, A. Pytlik, K. Pacześniowski, Analysis of Deformation of Mining Chains Based on Motion Tracking. In *International Symposium on Visual Computing*, 588-596, Springer, Berlin, Heidelberg, (2012, July).

[51] Directive 2014/34/EU of the European Parliament and of the Council of 26 February 2014 on the harmonisation of the laws of the Member States relating to equipment and protective systems intended for use in potentially explosive atmospheres (recast) (OJEU L 96, 29.3.2014, p. 309).

[52] S. Nowak, Elektryczne i nieelektryczne urządzenia (Ex). [Electrical and non-electrical devices (Ex)], Automatic Systems Engineering, Gdańsk, (2015).

[53] A. Pytlik, Identyfikacja możliwych źródeł zapłonu atmosfery wybuchowej podczas badań łańcuchów i stojaków ciernych przy obciążeniu dynamicznym. [Identifying potential explosive atmosphere ignition sources during the testing of chains and sliding joints under dynamic loading], in: S. Prusek, J. Knechtel, B. Madeja-Strumińska (Eds.), Zwalczanie zagrożeń aerologicznych w kopalniach. [Aerological hazard prevention in mines], joint publication, Główny Instytut Górnictwa, Katowice, 184-197 (2012).